

Charge transfer and excitation in slow 20 eV–2 keV $H^+ + D(1s)$ collisions

T G Lee, Anh-Thu Le and C D Lin

Department of Physics, Cardwell Hall, Kansas State University, Manhattan, KS 66506, USA

E-mail: ltg@phys.ksu.edu

Received 26 June 2003

Published 3 October 2003

Online at stacks.iop.org/JPhysB/36/4081

Abstract

We used the recently developed hyperspherical close-coupling method to study $H^+ + D(1s)$ collisions at H^+ impact energies between 20 eV and 2 keV. We showed that the cross sections for excitation and charge transfer to the 2p states are essentially identical over the whole energy range and stay relatively independent of energy from 2 keV down to about 150 eV. Below 150 eV the cross sections drop precipitously as the energy decreases. Electron capture to $H(1s)$ cross section in this energy region is also calculated.

(Some figures in this article are in colour only in the electronic version)

1. Introduction

Slow ion–atom collisions have been a subject of great interest for decades. The most elementary collision system $H^+ + H$ has attracted a great deal of interest from both theorists and experimentalists. Due to the difficulty of manipulating a low-energy ion beam, most of the experimental data have been taken at energies above about 1 keV. These experimental results, for energies between, say, about 10 and 500 keV, are relatively well described by the different theoretical approaches that have been developed over the last few decades [1, 2]. Between 1 and 10 keV, the major remaining issue, both theoretically and experimentally, is the total and differential impact ionization cross sections, see recent works in [3–7]. Ionization is a weak process below 10 keV and the cross section is small compared to the resonant charge transfer process. It is also small compared to excitation and charge transfer to the $n = 2$ states.

The focus of the present work is the collision of $H^+ + D(1s)$ from 2 keV down to about 20 eV. (The collision energy used in this paper refers to the H^+ impact energy in the laboratory, with the target initially at rest.) Here, not only are there details of just a few experiments available but the number of theoretical studies is also quite limited. In this energy regime, the dominant process is charge transfer to $H(1s)$ which is well understood since it differs little from the resonant charge transfer in $H^+ + H$ collisions. (Charge transfer for the latter process below 2 eV has been examined previously in papers [8, 9].) The next dominant process is the

excitation and charge transfer to $n = 2$ states. Existing calculations and experiments in the 2–10 keV region indicate that excitation and capture to the 2s state are much smaller and that the cross section drops rapidly as the collision energy decreases, see [10] for a summary of earlier references. On the other hand, excitation and charge transfer cross sections to 2p are larger and remain nearly constant in this energy range. One of the major motivations behind the present theoretical study is the question of whether the 2p cross section will begin to decrease at a certain energy and if so, at what energy.

Despite the great progress made in ion–atom collision theory over the past few decades, most of the effort has been focused in the higher energy region where the motion of the heavy particles can be treated classically. Using the impact parameter approach the time-dependent electronic wavefunction can be expanded in terms of either atomic orbitals or in terms of molecular orbitals (MOs). The latter is called the perturbed stationary state (PSS) approximation and was first proposed by Massey and Smith [11] in 1933. If the impact velocity is small in comparison with the typical speed of the electron then the PSS model is preferred. However, with the PSS model the molecular basis functions do not satisfy the correct asymptotic boundary condition and the calculated results are not Galilean invariant. To overcome this difficulty, various forms of electron translational factors or switching functions have been introduced [12–15]. These functions have also been extended to collisions at lower energies where semiclassical treatment fails and a quantum description of the motion of the heavy particles is needed. Similar switching functions or the more advanced reaction coordinates have been introduced in quantum theory [16–19]. Calculations based on such models are not founded on first principles since the switching functions or reaction coordinates have to be chosen in an *ad hoc* manner.

In view of these deficiencies, we have recently developed the hyperspherical close-coupling (HSCC) method to study low-energy ion–atom collisions [20]. No *ad hoc* parameters are used and the accuracy of the method can, in principle, be checked by increasing the number of channels included in the close-coupling calculations. The HSCC method has been applied to a few ion–atom collision processes so far [20–22]. In this work we present HSCC results for $H^+ + D(1s)$ collisions from 20 eV to 2 keV. In this energy region, the results are expected to be identical to $H^+ + H(1s)$ collisions. This paper is organized as follows. In section 2, we review briefly the HSCC method for ion–atom collisions. The results for the $H^+ + D(1s)$ reaction are presented in section 3. The summary and conclusions are given in section 4. Atomic units are used unless otherwise indicated.

2. Hyperspherical close-coupling theory

The details of the HSCC theory are given in Liu *et al* [20]. In the centre-of-mass frame we solved the time-independent Schrödinger equation for the three-body HD^+ system in the mass-weighted hyperspherical coordinates. Let $\vec{\rho}_1$ be the first Jacobi vector from D^+ to H^+ with reduced mass μ_1 and let $\vec{\rho}_2$ be the second Jacobi vector from the centre of mass of D^+ and H^+ to the electron with reduced mass μ_2 . The hyperradius R and hyperangle ϕ are defined as

$$R = \sqrt{\frac{\mu_1}{\mu} \rho_1^2 + \frac{\mu_2}{\mu} \rho_2^2}, \quad (1)$$

$$\tan \phi = \sqrt{\frac{\mu_2}{\mu_1} \frac{\rho_2}{\rho_1}}, \quad (2)$$

where μ is arbitrary. We further define angle θ to be the angle between the two Jacobi vectors. If we choose μ to be equal to μ_1 , then the hyperradius R is very close to the internuclear

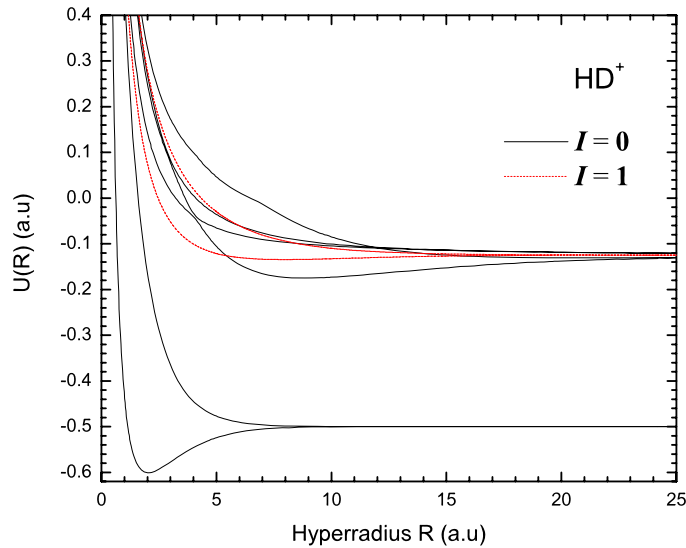


Figure 1. Adiabatic hyperspherical potential curves for HD⁺. The figure shows six $I = 0$ channels represented by solid curves and two $I = 1$ channels represented by dashed curves.

separation. By introducing the rescaled wavefunction

$$\Psi(R, \Omega, \hat{\omega}) = \psi(R, \Omega, \hat{\omega}) R^{3/2} \sin \phi \cos \phi, \quad (3)$$

we solve the Schrödinger equation in the form

$$\left(-\frac{1}{2} \frac{\partial}{\partial R} R^2 \frac{\partial}{\partial R} + \frac{15}{8} + H_{\text{ad}}(R, \Omega, \hat{\omega}) - \mu R^2 E \right) \Psi(R, \Omega, \hat{\omega}) = 0, \quad (4)$$

where $\Omega \equiv \{\phi, \theta\}$ and $\hat{\omega}$ denotes the three Euler angles of the body-fixed frame axes with respect to the space-fixed frame. H_{ad} is the adiabatic Hamiltonian with the hyperradius fixed. To solve equation (4), we expand the rescaled wavefunction as

$$\Psi(R, \Omega, \hat{\omega}) = \sum_{\nu} \sum_I F_{\nu I}(R) \Phi_{\nu I}(R; \Omega) \tilde{D}_{I M_I}^J(\hat{\omega}), \quad (5)$$

where ν is the channel index, J is the total angular momentum, I is the absolute value of the projection of \vec{J} along the body-fixed z' axis, taken to be the axis between the two heavy particles and M_I is the projection along the space-fixed z axis. In this equation, \tilde{D} is the normalized and symmetrized rotation function. The body-frame adiabatic basis functions $\Phi_{\mu I}(R; \Omega)$ are solutions of a two-dimensional partial differential equation in Ω which are solved in terms of B -spline functions. The resulting coupled hyperradial equations are solved using the R -matrix propagation method. Within each sector, the smooth variable discretization technique was used. We comment that the expansion (5) is very similar to the PSS expansion except that we use the hyperradius as the adiabatic parameter, instead of internuclear separation as in PSS theory.

In figure 1 we show the adiabatic hyperspherical potential curves for HD⁺ that converge to the $n = 1$ and 2 states of H and D. These eight adiabatic channels were used in the HSCC calculation, even though we will show that in the energy region of interest, calculations based only on four channels will be adequate. Within the accuracy shown in figure 1, these potential curves are essentially identical to the Born–Oppenheimer potential curves. In actuality, the two lowest curves are separated by about 3.7 meV, which is the energy difference between

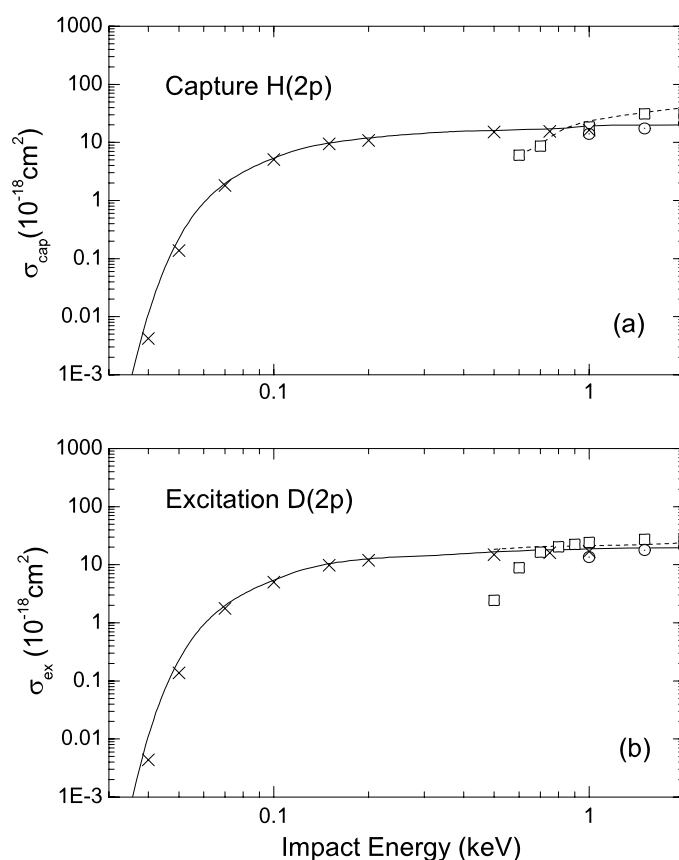


Figure 2. Comparison of the HSCC calculations with the experimental and semiclassical results available for $\text{H}^+ + \text{D}(1s)$ collisions. (a) Electron capture to the $\text{H}(2p)$ level: —, HSCC (eight channels); \times , HSCC (four channels); - - -, 3CAOCC; \odot , TDDFT; \square , ORNL [24]. (b) Same as (a) but for excitation to the $\text{D}(2p)$ level.

$\text{H}(1s)$ and $\text{D}(1s)$, since the HSCC method accounts for the mass effect, in contrast to the PSS method. Similarly, the excited state curves also converge to H or D $n = 2$ states.

The basic collision dynamics for the present system are well known. The two lowest curves have an avoided crossing near $R \simeq 12$ au [8], which is responsible for the charge transfer from $\text{D}(1s)$ to $\text{H}(1s)$. The upper curve of the pair, to be called $2p\sigma$, in analogy with the H_2^+ potential, is known to be rotationally coupled to the $2p\pi$ curve (the lowest $I = 1$ curve in figure 1) at small distances. This rotational coupling is responsible for populating the $2p$ state in $\text{H}^+ + \text{H}$ collisions—a fact already well understood from the semiclassical theory for collisions above 1–2 keV.

3. Results and discussion

From the present HSCC calculations using the eight channels shown in figure 1, we obtained electron capture to $\text{H}(2p)$ and excitation to $\text{D}(2p)$ cross sections. The results are shown in figure 2 as solid curves. Since the major mechanism for populating these states is rotational coupling, a four-state calculation including only the two lowest $I = 0$ and two lowest $I = 1$

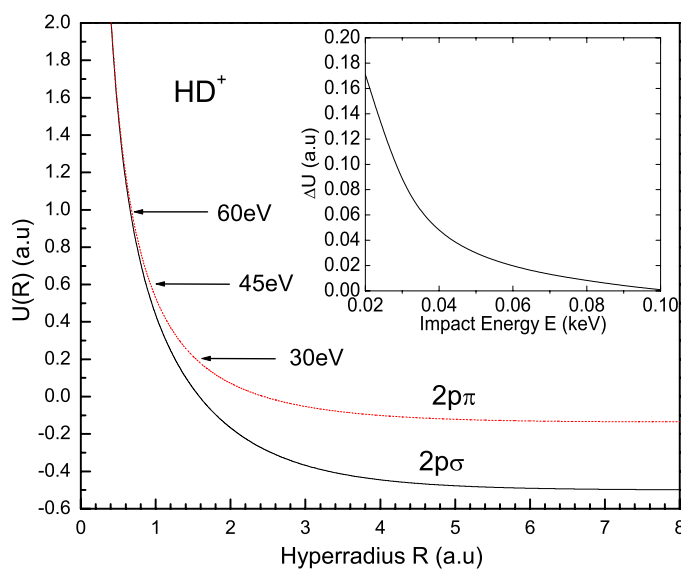


Figure 3. Adiabatic hyperspherical potential curves for $2p\sigma$ and $2p\pi$ states. The arrows indicate the position of the classical turning point of the $2p\pi$ curve at the given proton impact energy. The inset shows the energy difference between these two curves at the classical turning point as a function of proton impact energy.

states would give essentially the same results, as shown by crosses in figure 2. We also comment that the $2p$ states thus populated are almost pure $2p\pi$ states where the quantization axis is the incident beam direction. This is already the case for collision energies of about 2 keV, see table 1 of Fritsch and Lin [23].

Figure 2 shows the results that we were looking for. The $2p$ excitation or capture cross sections stay relatively constant until about 150 eV. From there they drop rapidly as the collision energy is reduced.

In figure 2 we also show other theoretical results and the unpublished experimental data from Barnett [24] at energies down to 500 eV. These experimental data show relatively large differences between excitation and capture to the $2p$ states. Based on the MO concept, and supported by the present HSCC calculation, there is no reason to expect that these two cross sections will differ in this energy region. It is noted that the cross sections for these two processes are known to be essentially the same in the 1–5 keV region [2]. Similarly, it is difficult to interpret the theoretical results from the three-centre atomic orbital close coupling (3CAOCC) calculations by McLaughlin *et al* [10] which show that the two cross sections differ markedly below 1 keV. Note that a similar earlier three-centre calculation by Winter and Lin [25] showed that the two cross sections are identical at 1.56 and at 3 keV to within a few percentage points. The recent semiclassical time-dependent density functional theory (TDDFT) result of Tong *et al* [26] did show that the two cross sections are very close to each other down to a collision energy of 1 keV. Their method used a straight line trajectory and may begin to incur errors at the lowest energy point shown.

To understand the rapid drop in the excitation and charge transfer cross sections to $2p$ states at low energies, as shown in figure 2, we display the $2p\sigma$ and $2p\pi$ potential curves in more detail in figure 3 in the small R region since the rotational coupling between these two curves is responsible for the transitions. The positions of the classical turning point for the $2p\pi$ curve for collision energies at 60, 45 and 30 eV are shown. In the inset the energy gap

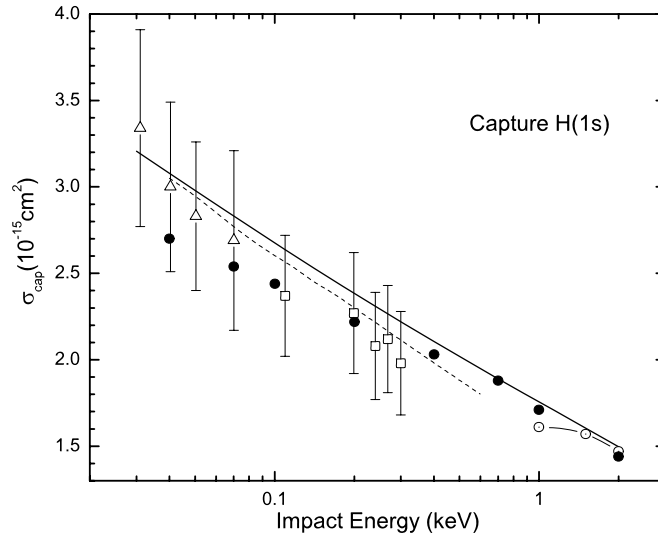


Figure 4. Comparison of the capture cross sections of H(1s) from HSCC with the existing experimental and theoretical results. —, HSCC; - - -, [27]; \circ , TDDFT [26]; \bullet , ORNL [24]; \triangle , H⁺ + D(1s) [28]; \square , H⁺ + H(1s) [28].

between the $2p\sigma$ and $2p\pi$ curves at the position of the classical turning point for the $2p\pi$ curve as functions of the impact energy is shown. This energy gap increases rapidly at lower impact energies, making transitions from $2p\sigma$ to $2p\pi$ via rotational coupling less and less efficient. At impact energies of 100 eV and higher, the energy gap is practically zero and the rotational coupling is efficient. The classical turning points in this figure were calculated for a zero total angular momentum. For higher total angular momenta, the turning points will be shifted to larger R values leading to larger energy gaps. Thus, the rapid drop in $2p$ excitation and charge transfer cross sections at lower energies can be understood based on adiabatic hyperspherical (or even Born–Oppenheimer) potential curves.

In the present calculations, we also obtained an electron capture cross section to H(1s). In figure 4 we compared the HSCC result with the earlier calculation of Dalgarno and Yadav [27], the recent (TDDFT) result of Tong *et al* [26] and the recommended data from the Oak Ridge National Laboratory (ORNL). We present partial-wave cross sections in terms of the impact parameter dependence probabilities according to the relationship

$$\sigma_J = \frac{2\pi bP(b)}{k}, \quad (6)$$

with $J = kb$, where k is the momentum. The results for the capture and excitation to the $2p$ states as well as the capture to H(1s) are shown in figures 5 and 6, respectively.

In figure 5, for high impact energies (i.e. 0.5 and 1 keV), the probabilities of capture to H(2p) and excitation to D(2p) differ by $\sim 3\%$. As the collision energy is decreased, the two probabilities practically lie on top of each other. Their general features do not differ much from those in the energy region of a few kiloelectronvolts [23, 25]. Namely, the probabilities for the excitation to D(2p) and charge transfer to H(2p) are *bell-shaped* functions of the impact parameters. In contrast, the H(1s) capture probability oscillates rapidly, and more so as the collision energy is decreased. We remark that the nonzero minima in the oscillatory electron capture probability in figure 6 for small impact parameters are the consequence of rotational coupling.

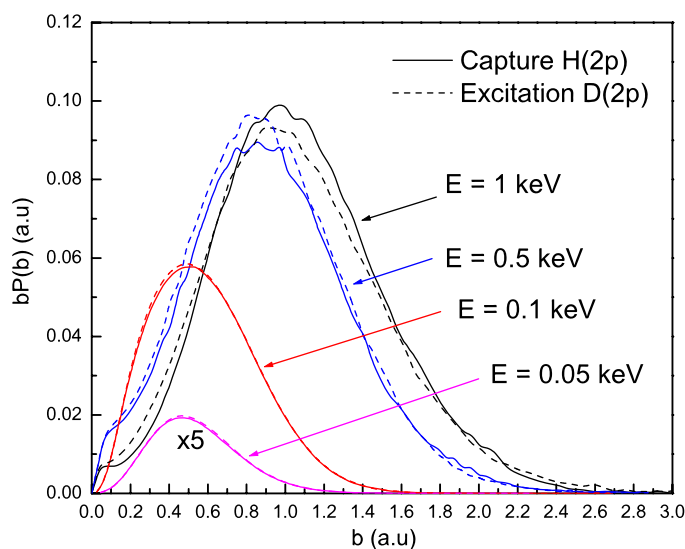


Figure 5. Impact parameter-weighted probabilities as functions of the impact parameter b for collision energies of $E = 0.05$ – 1 keV.

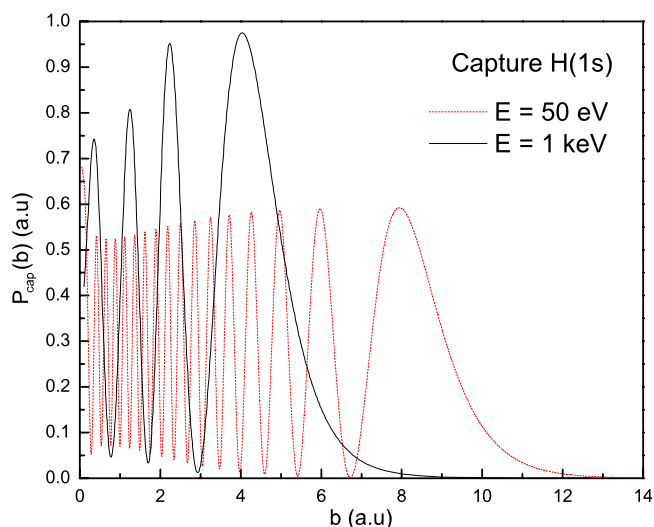


Figure 6. Electron capture probabilities as functions of the impact parameter b for collision energies of $E = 50$ eV and 1.0 keV.

4. Summary

In summary, we have employed the recently developed HSCC method to obtain excitation and charge transfer cross sections to $2p$ states in $H^+ + D$ (applicable to $H^+ + H$ also) collisions at energies from 20 eV to 2 keV. The two cross sections are shown to be essentially identical and remain nearly energy independent from 2 keV down to about 150 eV. Below that energy, the cross sections drop precipitously. The drop has been attributed to the increasingly larger energy gap between the $2p\sigma$ and $2p\pi$ curves in the classically allowed region, thus making the rotational coupling inefficient for populating the $2p$ state.

Acknowledgments

TGL would like to acknowledge the discussions with Dr M Hesse. This work was supported in part by the Chemical Sciences, Geosciences and Biosciences Division, Office of Basic Energy Sciences, Office of Science, US Department of Energy.

References

- [1] Bransden B H and McDowell M R C 1992 *Charge Exchange and Theory of Ion-Atom Collisions* (Oxford: Clarendon)
- [2] Fritsch W and Lin C D 1991 *Phys. Rep.* **202** 1
- [3] Sidky E, Illescas C and Lin C D 2000 *Phys. Rev. Lett.* **85** 1634
- [4] Schultz D R, Reinhold C O, Krstic P S and Strayer M R 2002 *Phys. Rev. A* **65** 052722
- [5] Macek J H and Ovchinnikov S Y 1998 *Phys. Rev. Lett.* **80** 2298
- [6] Shah M B, Geddes J, McLaughlin B M and Gilbody H B 1998 *J. Phys. B: At. Mol. Opt. Phys.* **31** L757
- [7] Piekma M, Ovchinnikov S Y, Van Eck J, Westerveld W and Niehaus A 1994 *Phys. Rev. Lett.* **73** 46
- [8] Igarashi A and Lin C D 1999 *Phys. Rev. Lett.* **83** 4041
- [9] Esry B D and Sadeghpour H R 1999 *Phys. Rev. A* **60** 3604
- [10] McLaughlin B M, Winter T G and McCann J F 1997 *J. Phys. B: At. Mol. Opt. Phys.* **30** 1043
- [11] Massey H S and Smith R A 1933 *Proc. R. Soc. A* **142** 142
- [12] Delos J B 1981 *Rev. Mod. Phys.* **53** 287
- [13] Thorson W R, Kimura M, Choi J H and Knudson S K 1981 *Phys. Rev. A* **24** 1768
- [14] Scheiderman S B and Russek A 1969 *Phys. Rev.* **181** 311
- [15] Vaanben J and Taulbjerg K 1981 *J. Phys. B: At. Mol. Phys.* **14** 1815
- [16] Errea L F, Harel C, Jouin H, Mendez L, Pons B and Riera A 1998 *J. Phys. B: At. Mol. Opt. Phys.* **31** 3527
- [17] Croft H and Dickinson A S 1996 *J. Phys. B: At. Mol. Opt. Phys.* **29** 57
- [18] Gargaud M, McCarroll R and Valiron P 1987 *J. Phys. B: At. Mol. Phys.* **20** 1555
- [19] Shimakura N and Kimura M 1991 *Phys. Rev. A* **44** 1659
- [20] Liu C N, Le A T, Morishita T, Esry B D and Lin C D 2003 *Phys. Rev. A* **67** 052705
- [21] Le A T, Liu C N and Lin C D 2003 *Phys. Rev. A* **68** 012705
- [22] Le A T, Hesse M, Lee T G and Lin C D 2003 *J. Phys. B: At. Mol. Opt. Phys.* **36** 3281
- [23] Fritsch W and Lin C D 1982 *Phys. Rev. A* **26** 762
- [24] Barnett C F 1990 *Oak Ridge National Laboratory Report* No 6086, unpublished
- [25] Winter T G and Lin C D 1984 *Phys. Rev. A* **29** 567
- [26] Tong X M, Kato D, Watanabe T and Ohtani S 2001 *Phys. Rev. A* **62** 052701
- [27] Dalgarno A and Yadav H N 1953 *Proc. R. Soc. A* **66** 173
- [28] Newman J H, Colgan J D, Ziegler D L, Nitz D E, Rundel R D, Smith K A and Stebbings R F 1982 *Phys. Rev. A* **25** 2976